Integrated Layout and Support Structure Optimization for Offshore Wind Farm Design

2016 J. Phys.: Conf. Ser. 753 092011

(http://iopscience.iop.org/1742-6596/753/9/092011)

Integrated Layout and Support Structure Optimization for Offshore Wind Farm Design

T Ashuri

Department of Mechanical Engineering, Arkansas Tech University, 1811 N Boulder Ave, Russellville, AR 72801, USA

E-mail: tashuri@atu.edu

C Ponnurangam, J Zhang and M Rotea

Department of Mechanical Engineering, University of Texas at Dallas, 800 W Campbell Rd, Richardson, TX 75080, USA

Abstract. This paper develops a multidisciplinary design optimization framework for integrated design optimization of offshore wind farm layout and support structure. A computational model is developed to characterize the physics of the wind farm wake, aerodynamic and hydrodynamic loads, response of the support structure to these loads, soil-structure interaction, as well as different cost elements. Levelized cost of energy is introduced as the objective function. The design constraints are the farm external boundary, and support structure buckling, first modal-frequency, fatigue damage and ultimate stresses. To evaluate the effectiveness of the proposed approach, four optimization scenarios are considered: a feasible baseline design, optimization of layout only, optimization of support structure only, and integrated design of the layout and support structure. Compared to the baseline design, the optimization results show that the isolated support structure design reduces the levelized cost of energy by 0.6%, the isolated layout design reduces the levelized cost of energy by 2.0%, and the integrated layout and support structure design reduces the levelized cost of energy by 2.6%.

1. Introduction

In recent years, wind energy has evolved as a reliable source of clean energy among all the other renewables [1–6]. However, the cost of wind energy generation is in general higher compared to the conventional energy resources, particularly for offshore wind [7, 8]. To make wind energy cost competitive, its levelized cost of energy (LCOE) has to be reduced further. For offshore applications, support structure is a major cost contributor [9–13].

The current practice in designing the support structure is based on a fixed layout [14–18]. The wind farm layout is optimized first, followed by the design of the support structure. This isolated approach generally results in a suboptimal design of both the layout and support structure, and it may increase the cost. An integrated layout and support structure design is expected to reduce the cost, by optimizing the layout and support structure simultaneously.

This paper develops a methodology for integrated wind farm optimization of the layout and support structure. A comprehensive computational code is developed for offshore wind farm multidisciplinary design optimization that consists of both modeling and optimization. A series

of models are developed to characterize the physics of the wind farm, including the Jensen model for wakes [19, 20], a blade element momentum model (BEM) for aerodynamic loads [21], an annual energy production model [22], a structural model for the support structure and its interaction with soil [16, 23], a hydrokinematic model for waves [24], and Morisons equation for hydrokinetic loads on the support structure [25, 26]. The LCOE is computed based on different cost elements of the wind farm including the turbine capital costs, levelized replacement costs, operational and maintenance costs, cabling costs, cost of labor, scour protection, and installation cost. Since these cost models are confidential, only normalized cost data are presented in the paper. Sequential quadratic programing, a gradient-based optimization algorithm, is adopted to solve this multidisciplinary problem. The objective function is the LCOE with side constraints on the land use, support structure buckling, first modal-frequency, fatigue damage, and stresses.

To show the effectiveness of the proposed approach, four wind farm design scenarios are considered. First, a baseline design is developed that has a feasible support structure design with 7D equal spacing between rows and columns. The baseline design is not optimal for the given layout, and it serves as a basis to compare different optimization scenarios in a relative manner. Second, a wind farm layout optimization of the baseline design is performed without optimizing the support structure design variables. Third, the support structure of the baseline design is optimized for a spacing of 7D. Fourth, an integrated layout and support structure optimization is performed to minimize the LCOE. The wind farm consists of 100 Vestas V80 turbines with a 10x10 layout arrangement. Results of these four cases are analyzed and compared to evaluate the effectiveness of the integrated layout and support structure design. This also allows to make a comparison between different optimization scenarios and their individual impact on LCOE.

2. Methodology

Multidisciplinary feasible (MDF) architecture is used to optimize the LCOE [27] as depicted in Figure 1. In the MDF architecture, the optimizer is directly coupled to a multidisciplinary analysis model. The design variables are passed to the disciplinary analysis models, which compute the design constraints and the objective function of the coupled system. Then, the objective and design constraints are passed back to be evaluated by the optimizer. This iterative approach continues until 1% convergence is achieved between two consecutive iterations for the LCOE. Next subsection explains the multidisciplinary analysis models and the optimization setup.

2.1. Multidisciplinary analysis models

The Jensen wake model [28, 29] is used to determine the velocity deficit and wake diameter in the wind farm. The wake expansion diameter (D_W) behind the downstream wind turbine is calculated as:

$$D_w = D(1 + 2ks) \tag{1}$$

where, D is the wind turbine rotor diameter, k is the wake decay coefficient with a value of 0.4, and s is the downstream distance from the wind turbine. The velocity deficit (Δu) for a fully developed wake condition is given as:

$$\Delta u = U_\infty \frac{(1 - \sqrt{1 - C_T})}{(1 + 2ks)^2} \tag{2}$$

where C_T is the thrust coefficient having a value of 0.7, and U_∞ is the wind speed measured at the hub height. BEM is used to compute the power output and the aerodynamic loads from the cut-in to cut-out wind speeds for each turbine in the wind farm. This allows the computation of the annual energy production in the wind farm as [30]:

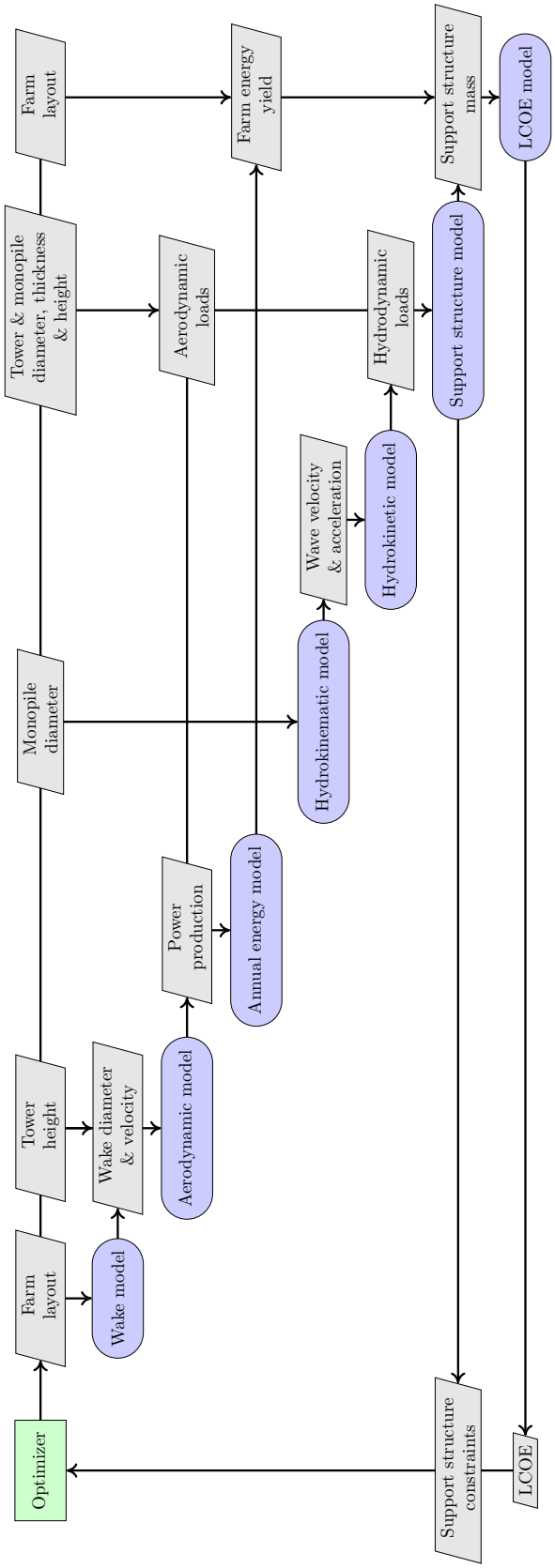

Figure 1: Offshore wind farm design optimization architecture. The arrows show the direction of the data flow and the data dependency.

$$AEP = 8760 \sum_{j=1}^{n} \sum_{i=cut-in}^{cut-out} P_j(v_i) f(v_i) \tag{3}$$

where 8760 is the number of hours in a year, j is the number of wind turbines in the farm, i is the discrete wind speed bin v from the cut-in to cut-out, $P_j(v_i)$ is the power output of turbine j at wind speed i that is computed using the BEM model, and $f(v_i)$ is Weibull portability function at wind speed i defined as [30]:

$$f(v_i) = \left(\frac{k}{c}\right)\left(\frac{v_i}{c}\right)^{k-1} \exp\left[-(\frac{v_i}{c})^k\right] \tag{4}$$

where k is the Weibull shape factor and c is the scale factor.

In addition to the aerodynamic loads acting on the rotor and tower, the impact of hydrodynamic loads is also considered, since it is crucial in designing the support structure. Wave kinematics are modeled using Airy's wave theory [31]. Airy theory provides wave kinematics up to the mean sea surface. Wheeler stretching technique is used to redistribute the velocity and acceleration profiles up to the actual sea surface [32]. The hydrodynamic loads to compute the drag (f_{Drag}) and inertia ($f_{Inertia}$) forces on the submerged part of the transition piece and monopile are based on Morison's equation [33], given by:

$$f_{Morison} = f_{Drag} + f_{Inertia} = \frac{1}{2}\rho C_d \mid U \mid U + \frac{\pi D^2}{4}\rho C_m \dot{U} \tag{5}$$

where, ρ is the density of water, D is the outer diameter of the monopile, U and $\dot{U}$ are the respective velocity and acceleration in horizontal fluid plane, and C_d and C_m are coefficients of drag and inertia, respectively.

The support structure is modeled using Timoshenko beam-element theory [34]. Discretization is performed at different sections along the height as presented in Figure 2 to allow variation in properties. Each section is represented as an element with two nodes and six degrees of freedom. The soil is modelled as a series of lateral springs that are added to the structural stiffness. This allows capturing the soil-structure interaction of the monopile below the mud-line [35,36]. Linear interpolation is used to find the soil stiffness at the location of the finite element nodes of the monopile.

2.2. Optimization setup

The wind turbine chosen for this case study is the Vestas V80. Table 1 presents the gross properties of the wind turbine. Optimization is performed for wind speeds from the cut-in to cut-out wind speeds. Using the computed AEP from Equation 3, the $LCOE$ is calculated as:

$$LCOE = \frac{[(TCC + BOS) * IR] + DEC + O\&M}{AEP} \tag{6}$$

where TCC is the turbine capital cost that consists of rotor-nacelle assembly, and tower; BOS is the balance of station cost and it consists of foundation, site permits and engineering, wind farm electrical systems, and installation; IR is the interest rate; DEC is the wind turbine and wind farm decommissioning costs; and $O\&M$ is the operation and maintenance costs [37].

The foundation cost comprises the transition piece, boat landing, grout connection, and monopile. The wind farm electrical systems cost includes the infield cabling, transmission cable to shore, shunt reactor, transformer, and switch gear. The installation cost accounts for the support structure, rotor-nacelle assembly, electrical infrastructure, and harbor use. The decommissioning costs covers the removal of the wind turbine and wind farm infrastructure. The administrative, bottom lease, grid change, and insurance cost come under the operation

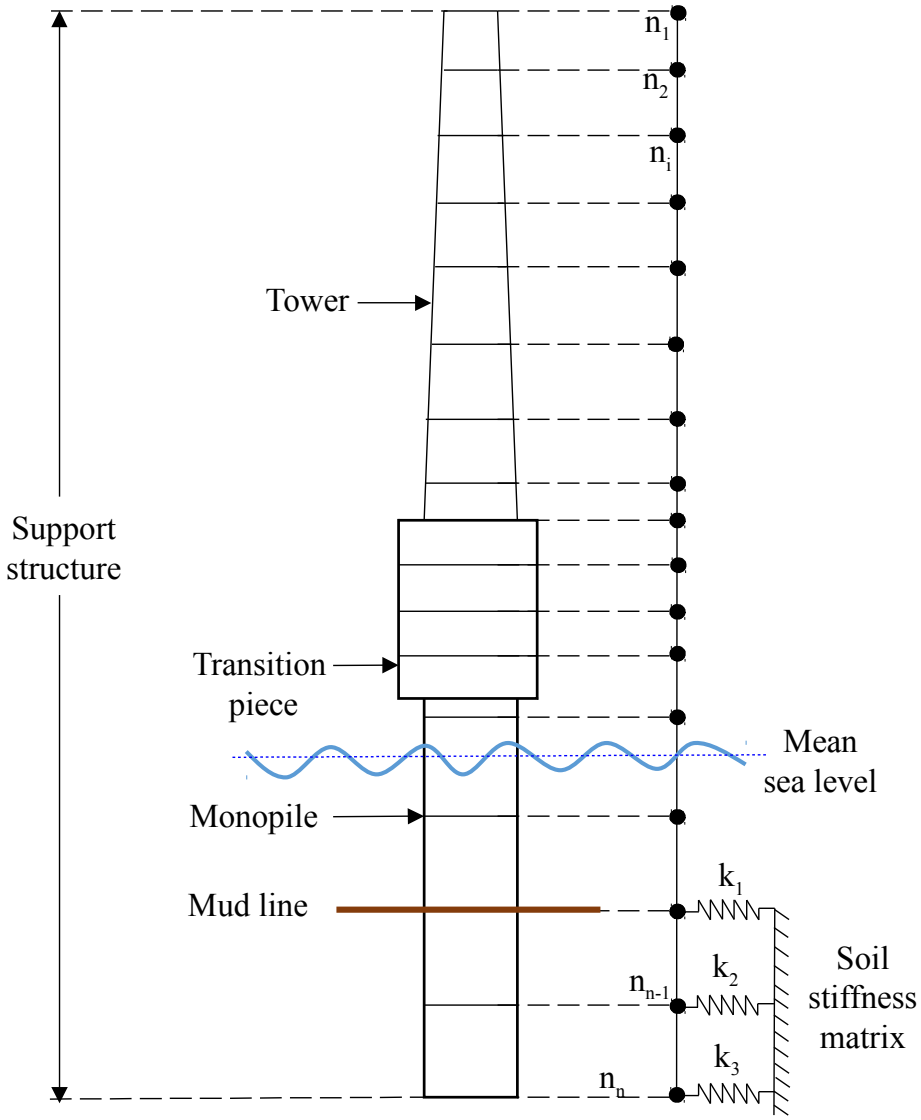

Figure 2: Schematic diagram of the support structure model

costs. The maintenance costs include the management of crew and personnel, access vessels, lifting equipment, sub-sea inspection, and service and repair.

In Equation 6, the costs of tower and foundation, wind farm electrical infrastructure, and AEP are not fixed, due to their dependency to the layout. For the support structure, the impact of hydrodynamic loads acting on the monopile is considered through the wave kinematics and kinetics, as well as the aerodynamic loading acting on the rotor and tower.

The design variables used for this optimization study are the wind farm layout, and the support structure height, diameter, and thickness. Hence, the optimization problem formulation

Table 1: Vestas V80 wind turbine properties.

Properties	Value
Power regulation	Pitch controlled
Power maximization	Variable speed
Rated power	2 MW
IEC class	1A
Cut-in wind speed	4 m/s
Rated wind speed	14 m/s
Cut-out wind speed	25 m/s
Rotor diameter	80 m
Number of blades	3

Source:`http://www.thewindpower.net/turbine_en_29_vestas_1800.php` last retrieved June 11, 2016.

is mathematically expressed as:

$$\min \text{LCOE subject to} \quad \mathbf{h_k} \leq 0 \Rightarrow \begin{cases} h_1 \leq 0 \\ h_2 \leq 0 \\ \vdots \\ h_k \leq 0 \end{cases} \tag{7}$$

where $\mathbf{h_k}$ is the vector of design constraints.

For the support structure, the design constraints are the buckling loads, fatigue damage, first modal-frequency, and ultimate stresses. Both the local and global buckling are considered in this study. Fatigue damage is computed by applying a rainflow cycle counting of the stress time signals, followed by the Miner rule [38–40]. Fatigue properties are defined by the slope of the S-N curve, and the static stress. For the entire support structure, a slope of 5 and an intercept of 110 MPa are considered.

Sequential quadratic programing is adopted as the optimization algorithm with interior and exterior penalty functions based on the feasibility of the design. The optimization problem can be formulated either as isolated or integrated. In the isolated approach, either the optimization of the support structure or the layout is performed. Optimization of the support structure aims at satisfying all the design constraints, and minimizing the mass of the support structure. Optimization of the layout aims to minimize the LCOE by optimizing the spacing. For the integrated design, both the support structure and layout design variables are optimized simultaneously (the isolated approach is not used here). The computational codes developed for this study are paralleled codes using MPI for Python [41]. The computation is performed on a 16 cores workstation ranging from 30 minutes to 2 hours depending on the optimization scenario considered.

3. Results

This section presents the results for an offshore wind farm consisting of 100 Vestas V80 turbines. The baseline layout arrangement is 10x10 with an initial wind turbine spacing of 7D between rows and columns. The water depth is 13.5 m, the significant wave height for 1 year and 50 year periods are 3.3 m and 5.0 m, respectively. Distance to harbor is 20 km.

Figure 3 presents the thickness distribution of the baseline, the integrated optimization, and the isolated support structure optimization along the support structure length, from the pile-tip to tower-top.

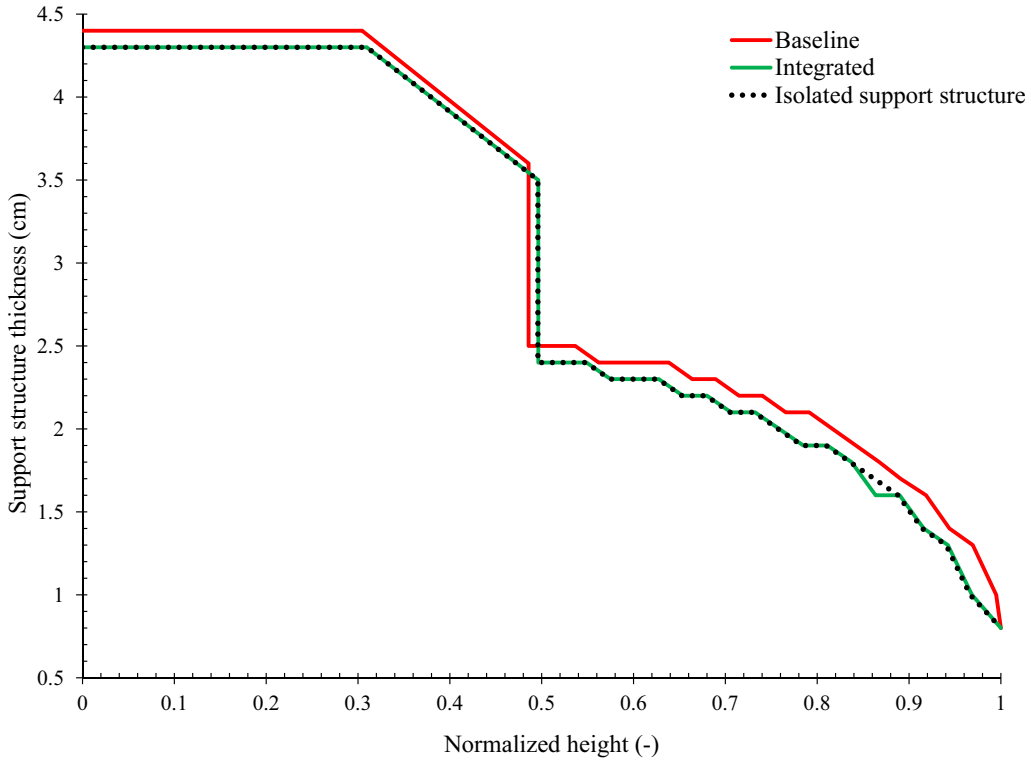

Figure 3: Thickness distribution along the height of the support structure.

In this figure, the isolated layout design is not shown since the same support structure as the baseline is used. As the figure shows, the integrated design and the isolated support structure design exhibit similar thickness distribution, but they both show significant improvement, with respect to the baseline design.

Similar to Figure 3, Figure 4 depicts the diameter distribution along the support structure length. Both the integrated and the isolated support structure design show considerable reductions in the diameter.

Figure 5 compares the location of the turbines for the baseline design, the isolated layout design, and the integrated layout and support structure design. It should be noted that the isolated support structure design has the same coordinates as the baseline design, and therefore is not shown. As the figure shows, the spacing of the isolated layout and integrated design has increased compared to the baseline. This is beneficial for energy capture, since the wake recovery is higher, but it impacts other cost elements as well.

Table 2 compares different cost elements for different designs. Since the isolated layout design uses the same support structure as the baseline design, it has the same hub height and TCC. However, during the optimization of the isolated layout the spacing between different turbines increases. This results in a higher wake efficiency of 3.59% with respect to the baseline design, and it thereby increases the AEP by 2.82%. Because of a wider spacing, the BOS and DEC costs increase as well, but overall the LCOE reduces by 1.97% compared to the baseline design.

For the isolated support structure design, the hub height reduces by 3.78%. This in turn decreases BOS, DEC and O&M costs. The wake efficiency remains the same, but since the hub

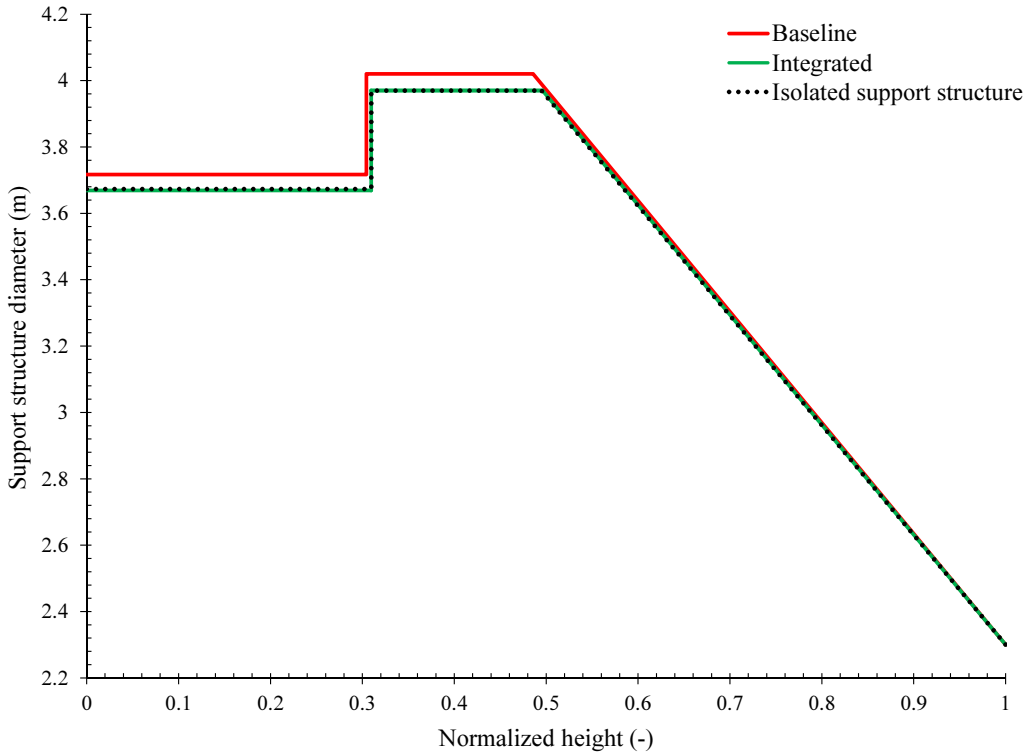

Figure 4: Diameter distribution along the height of the support structure.

height experiences a reduction, the AEP reduces as well. For this design, 0.6% reduction in the LCOE is obtained due to optimizing the support structure design, while using the same layout as the baseline design.

The integrated layout and support structure design experiences 4.11% reduction in its hub height. This negatively impacts the AEP, but due to a larger spacing between wind turbines, it is positively compensated by higher wake efficiency of 3.6% with respect to the baseline design. Due to a reduction of the hub height for this design, the BOS reduces by 0.09%, DEC by 0.86%, and O&M costs by 0.57%. In this case, the best trade-off between the support structure design and the layout enables a reduction of 2.62% for the LCOE.

Table 2: Comparison of different designs normalized with respect to the baseline design.

	Baseline	Isolated layout (%)	Isolated support structure (%)	Integrated layout & support structure (%)
Hub height	—	0.00	-3.78	-4.11
TCC	—	0.00	-0.72	-0.79
BOS	—	1.34	-2.13	-0.09
DEC	—	1.40	-2.09	-0.86
O&M	—	-0.14	-5.08	-0.57
AEP	—	2.82	-1.17	2.25
Wake efficiency	—	3.59	0.00	3.60
LCOE	—	-1.97	-0.60	-2.62

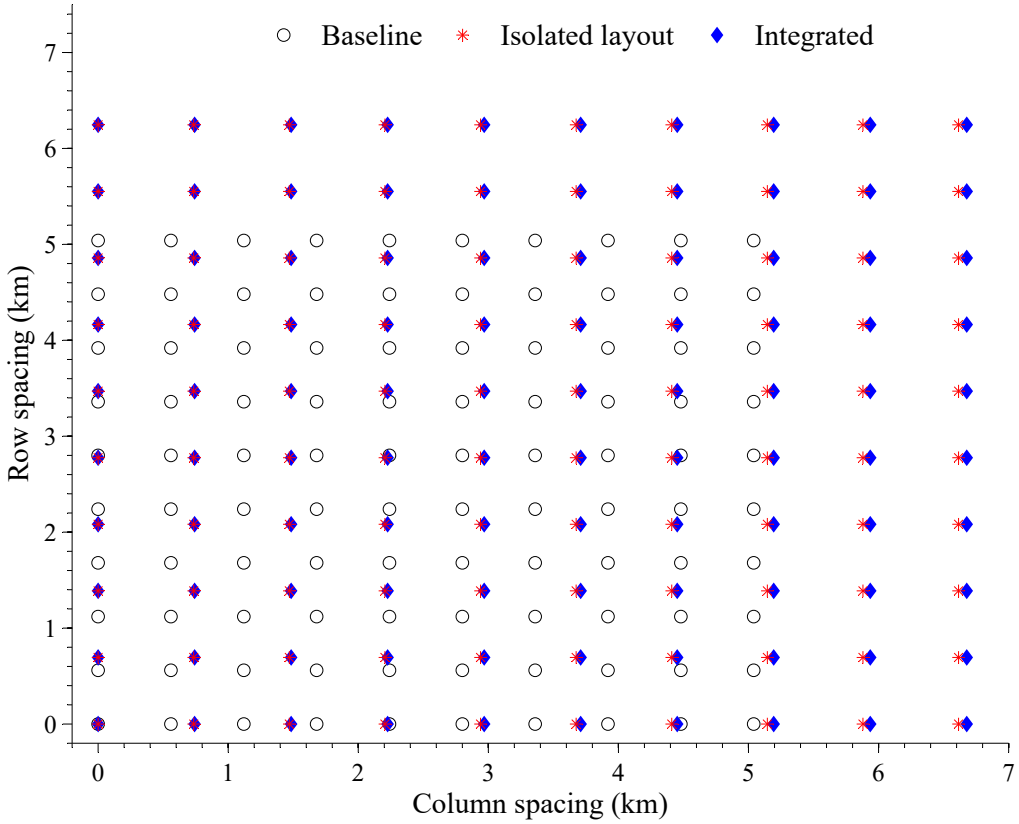

Figure 5: Spacing between the turbines in the offshore wind farm.

Figure 6 depicts the cost share of different elements for all the designs, and it is complementary to Table 2. For all design scenarios considered in this paper, the cost share of BOS is almost half of the total cost to construct, maintain, and decommission the wind farm. TCC has the second highest cost share with about 35% of the total cost.

4. Conclusion

The aim of this research was to identify the potential of integrated layout and support structure design optimization of offshore wind farms. A multidisciplinary design optimization framework was developed, which enables the integrated design optimization of offshore wind farm layout and support structure. A suite of computational models is developed to characterize the physics of the wind farm wake, aerodynamics and hydrodynamics loads, response of the support structure to these loads, soil-structure interaction, as well as different cost elements. The integrated design approach was compared to three other cases, including a feasible baseline design, an isolated layout design, and an isolated support structure design.

Results showed that an integrated design of both layout and support structure can reduce the LCOE by 2.6% with respect to the baseline design. This shows the importance of integrated design of the offshore support structure and layout. An isolated optimization of the layout or support structure does not take into account the coupling between these two, hence, it is only possible to find the best design by a trade-off between the layout and support structure.

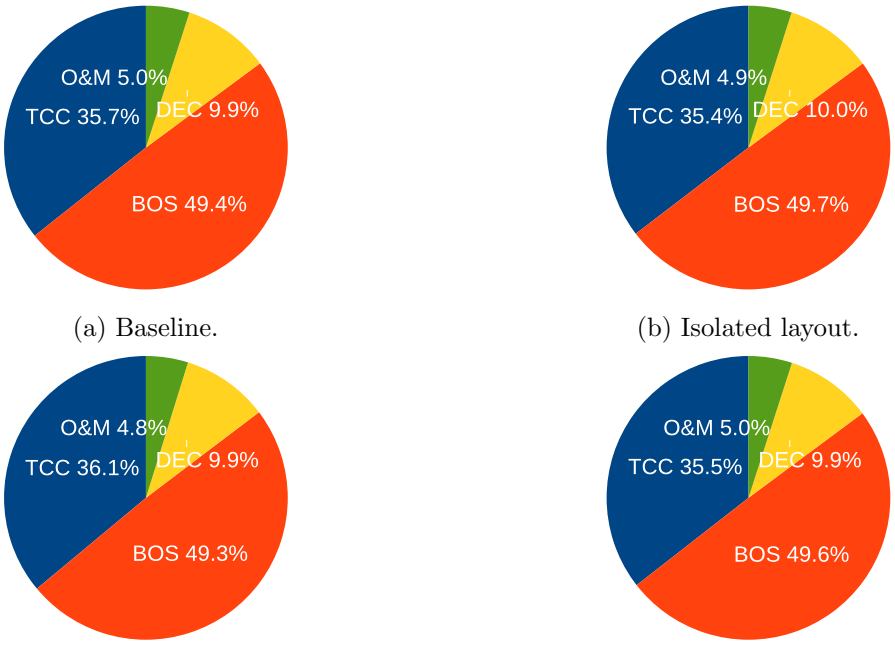

(a) Baseline. (b) Isolated layout.

(c) Isolated support structure. (d) Integrated.

Figure 6: Share of different cost elements for all designs.

5. References

[1] Ellabban O, Abu-Rub H, Blaabjerg F. Renewable energy resources: Current status, future prospects and their enabling technology. Renewable and Sustainable Energy Reviews. 2014;39:748–764.
[2] Sobhansarbandi S, Atikol U. Performance of Flat-Plate and Compound Parabolic Concentrating Solar Collectors in Underfloor Heating Systems. Journal of Solar Energy Engineering. 2015;137(3):034501.
[3] López I, Andreu J, Ceballos S, de Alegría IM, Kortabarria I. Review of wave energy technologies and the necessary power-equipment. Renewable and Sustainable Energy Reviews. 2013;27:413–434.
[4] Ashuri T, Bussel G, Mieras S. Development and validation of a computational model for design analysis of a novel marine turbine. Wind Energy. 2013;16(1):77–90.
[5] Papadimitratos A, Sobhansarbandi S, Pozdin V, Zakhidov A, Hassanipour F. Evacuated tube solar collectors integrated with phase change materials. Solar Energy. 2016;129:10–19.
[6] Ashuri T, Zaaijer MB, Martins JR, Zhang J. Multidisciplinary design optimization of large wind turbines–Technical, economic, and design challenges. Energy Conversion and Management. 2016;123:56–70.
[7] Sun X, Huang D, Wu G. The current state of offshore wind energy technology development. Energy. 2012;41(1):298–312.
[8] Blanco MI. The economics of wind energy. Renewable and Sustainable Energy Reviews. 2009;13(6):1372–1382.
[9] Lozano-Minguez E, Kolios AJ, Brennan FP. Multi-criteria assessment of offshore wind turbine support structures. Renewable Energy. 2011;36(11):2831–2837.
[10] Ashuri T, Zaaijer MB. Review of design concepts, methods and considerations of offshore wind turbines. In: European Offshore Wind Conference and Exhibition, Berlin, Germany. European Wind Energy Association; 2007. p. 1–10.
[11] Elkinton CN, Manwell JF, McGowan JG. Offshore wind farm layout optimization (OWFLO) project: Preliminary results. University of Massachusetts. 2006;.
[12] Breton SP, Moe G. Status, plans and technologies for offshore wind turbines in Europe and North America. Renewable Energy. 2009;34(3):646–654.
[13] Ashuri T. Beyond classical upscaling: integrated aeroservoelastic design and optimization of large offshore wind turbines. PhD Thesis, Delft University of Technology; 2012.
[14] Muskulus M, Schafhirt S. Design optimization of wind turbine support structures-a review. Journal of Ocean and Wind Energy. 2014;1(1):12–22.
[15] Pasamontes LB, Torres FG, Zwick D, Schafhirt S, Muskulus M. Support Structure Optimization for Offshore

Wind Turbines With a Genetic Algorithm. In: ASME 2014 33rd International Conference on Ocean, Offshore and Arctic Engineering. American Society of Mechanical Engineers; 2014. p. V09BT09A033.
[16] Haghi R, Ashuri T, van der Valk PL, Molenaar DP. Integrated multidisciplinary constrained optimization of offshore support structures. Journal of Physics: Conference Series. 2014;555(1):012046.
[17] Chew KH, Tai K, Ng E, Muskulus M. Optimization of Offshore Wind Turbine Support Structures Using an Analytical Gradient-based Method. Energy Procedia. 2015;80:100–107.
[18] Samorani M. The wind farm layout optimization problem. In: Handbook of Wind Power Systems. Springer; 2013. p. 21–38.
[19] Choi J, Shan M. Advancement of Jensen (Park) wake model. In: Proceedings of the European Wind Energy Conference and Exhibition; 2013. p. 1–8.
[20] Chowdhury S, Zhang J, Messac A, Castillo L. Unrestricted wind farm layout optimization (UWFLO): Investigating key factors influencing the maximum power generation. Renewable Energy. 2012;38(1):16–30.
[21] Sant T. Improving BEM-based aerodynamic models in wind turbine design codes. PhD Thesis, Delft University of Technology; 2007.
[22] Ashuri T, Rotea M, Xiao Y, Li Y, Ponnurangam CV. Wind Turbine Performance Decline and its Mitigation via Extremum Seeking Controls. In: AIAA Science and Technology Forum and Exposition (SciTech), Wind Energy Symposium, San Diego, California. American Institute of Aeronautics and Astronautics; 2016. p. 1–11.
[23] Ashuri T, Van Bussel G, Zaaijer M, Van Kuik G. An analytical model to extract wind turbine blade structural properties for optimization and up-scaling studies. In: The Science of making Torque from Wind, Heraklion, Crete, Greece; 2010. p. 1–7.
[24] Van der Meulen MB, Ashuri T, Van Bussel GJ, Molenaar DP. Influence of nonlinear irregular waves on the fatigue loads of an offshore wind turbine. In: The Science of Making Torque from Wind, Oldenburg , Germany. European Academy of Wind Energy; 2012. p. 1–10.
[25] Savenije L, Ashuri T, Van Bussel G, Staerdahl J. Dynamic modeling of a spar-type floating offshore wind turbine. In: European Wind Energy Conference & Exhibition, Warsaw, Poland. The European Wind Energy Association; 2010. p. 1–10.
[26] Naess A. Prediction of extremes of Morison-type loadingan example of a general method. Ocean Engineering. 1983;10(5):313–324.
[27] Martins JR, Lambe AB. Multidisciplinary design optimization: a survey of architectures. AIAA journal. 2013;51(9):2049–2075.
[28] Katic I, Højstrup J, Jensen NO. A simple model for cluster efficiency. In: European Wind Energy Association Conference and Exhibition; 1986. p. 407–410.
[29] Chowdhury S, Zhang J, Messac A, Castillo L. Optimizing the arrangement and the selection of turbines for wind farms subject to varying wind conditions. Renewable Energy. 2013;52:273–282.
[30] Ashuri T, Zaaijer MB, Martins JR, Van Bussel GJ, Van Kuik GA. Multidisciplinary design optimization of offshore wind turbines for minimum levelized cost of energy. Renewable Energy. 2014;68:893–905.
[31] Le Roux J. An extension of the Airy theory for linear waves into shallow water. Coastal Engineering. 2008;55(4):295–301.
[32] Wheeler J. Methods for calculating forces produced on piles in irregular waves. Journal of Petroleum Technology. 1970;1:1–2.
[33] Li Y, Yu YH. A synthesis of numerical methods for modeling wave energy converter-point absorbers. Renewable and Sustainable Energy Reviews. 2012;16(6):4352–4364.
[34] Nelson H. A finite rotating shaft element using Timoshenko beam theory. Journal of mechanical design. 1980;102(4):793–803.
[35] Nogami T, Otani J, Konagai K, Chen HL. Nonlinear soil-pile interaction model for dynamic lateral motion. Journal of Geotechnical Engineering. 1992;118(1):89–106.
[36] Matsunaga H. Vibration and buckling of deep beam-columns on two-parameter elastic foundations. Journal of sound and vibration. 1999;228(2):359–376.
[37] Scheu M, Matha D, Hofmann M, Muskulus M. Maintenance strategies for large offshore wind farms. Energy Procedia. 2012;24:281–288.
[38] Hashin Z. A reinterpretation of the Palmgren-Miner rule for fatigue life prediction. Journal of Applied Mechanics. 1980;47(2):324–328.
[39] Zwick D, Muskulus M. Simplified fatigue load assessment in offshore wind turbine structural analysis. Wind Energy. 2016;19(2):265–278.
[40] Muskulus M. Simplified rotor load models and fatigue damage estimates for offshore wind turbines. Philosophical Transactions of the Royal Society of London A: Mathematical, Physical and Engineering Sciences. 2015;373(2035):20140347.

[41] Dalcín L, Paz R, Storti M, DElía J. MPI for Python: Performance improvements and MPI-2 extensions. Journal of Parallel and Distributed Computing. 2008;68(5):655–662.